International Journal of Antimicrobial Agents 64 (2024) 107278

Contents lists available at ScienceDirect

International Journal of Antimicrobial Agents

journal homepage: www.elsevier.com/locate/ijantimicag

The novel drug candidate VOMG kills *Mycobacterium abscessus* and other pathogens by inhibiting cell division

Giulia Degiacomi[a,†], Laurent R. Chiarelli[a,†], Olga Riabova[b,†], Nicola Ivan Loré[c,†], Lara Muñoz-Muñoz[d,†], Deborah Recchia[a], Giovanni Stelitano[a], Umberto Postiglione[a], Fabio Saliu[c], Anna Griego[e,f], Viola Camilla Scoffone[a], Elena Kazakova[b], Edoardo Scarpa[e,f], José Manuel Ezquerra-Aznárez[d], Alessandro Stamilla[a], Silvia Buroni[a], Enrico Tortoli[c], Loris Rizzello[e,f], Davide Sassera[a,g], Santiago Ramón-García[d,h,i], Daniela Maria Cirillo[c], Vadim Makarov[b], Maria Rosalia Pasca[a,g,*]

[a] *Department of Biology and Biotechnology 'Lazzaro Spallanzani', University of Pavia, Pavia, Italy*
[b] *Federal Research Centre 'Fundamentals of Biotechnology' of the Russian Academy of Sciences, Moscow, Russia*
[c] *Emerging Bacterial Pathogens Unit, Division of Immunology, Transplantation and Infectious Disease, IRCCS San Raffaele Scientific Institute, Milan, Italy*
[d] *Department of Microbiology/Faculty of Medicine, University of Zaragoza, Zaragoza, Spain*
[e] *Department of Pharmaceutical Sciences, University of Milan, Milan, Italy*
[f] *National Institute of Molecular Genetics, Milan, Italy*
[g] *Fondazione IRCCS Policlinico San Matteo, Pavia, Italy*
[h] *Research and Development Agency of Aragon Foundation, Zaragoza, Spain*
[i] *Spanish Network for Research on Respiratory Diseases, Carlos III Health Institute, Madrid, Spain*

ARTICLE INFO

Article history:
Received 5 April 2024
Accepted 16 July 2024

Editor: Dr Renu Bharadwaj

Keywords:
Mycobacterium abscessus
Cell division
FtsZ
Non-tuberculous mycobacterium

ABSTRACT

Aims: The incidence of lung infections is increasing worldwide in individuals suffering from cystic fibrosis and chronic obstructive pulmonary disease. *Mycobacterium abscessus* is associated with chronic lung deterioration in these populations. The intrinsic resistance of *M. abscessus* to most conventional antibiotics jeopardizes treatment success rates. To date, no single drug has been developed targeting *M. abscessus* specifically. The objective of this study was to characterize VOMG, a pyrithione-core drug-like small molecule, as a new compound active against *M. abscessus* and other pathogens.
Methods: A multi-disciplinary approach including microbiological, chemical, biochemical and transcriptomics procedures was used to validate VOMG as a promising anti-*M. abscessus* drug candidate.
Results: To the authors' knowledge, this is the first study to report the *in-vitro* and *in-vivo* bactericidal activity of VOMG against *M. abscessus* and other pathogens. Besides being active against *M. abscessus* biofilm, the compound showed a favourable pharmacological (ADME-Tox) profile. Frequency of resistance studies were unable to isolate resistant mutants. VOMG inhibits cell division, particularly the FtsZ enzyme.
Conclusions: VOMG is a new drug-like molecule active against *M. abscessus*, inhibiting cell division with broad-spectrum activity against other microbial pathogens.

1. Introduction

Mycobacterium abscessus subsp. *abscessus* (*Mab*, also known as *Mycobacteroides abscessus* subsp. *abscessus*) is an opportunistic pathogen that has emerged recently as responsible for a wide range of clinical manifestations [1–3]. The incidence of *Mab*-induced pulmonary infections is increasing worldwide, and deserves particular attention in people with cystic fibrosis (CF) and chronic obstructive pulmonary disease (COPD) [4,5].

* Corresponding author at: M.R. Pasca, Department of Biology and Biotechnology 'Lazzaro Spallanzani', University of Pavia, via Ferrata 9, 27100 Pavia, Italy.
E-mail addresses: santiramon@unizar.es (S. Ramón-García), cirillo.daniela@hsr.it (D.M. Cirillo), makarov@inbi.ras.ru (V. Makarov), mariarosalia.pasca@unipv.it (M.R. Pasca).
† These authors contributed equally to this work.

https://doi.org/10.1016/j.ijantimicag.2024.107278

Mab is intrinsically resistant to many drugs, mainly due to the presence of a mycobacterial cell wall with low permeability. It is primarily composed of lipids, such as mycolic acids (up to 60%) [6]. Furthermore, unlike *Mycobacterium tuberculosis (Mtb), Mab* is characterized by two morphotypes: smooth and rough [6]. In *Mab* pulmonary infections, smooth strains producing glycopeptidolipids first colonize the lung epithelium and form biofilm [3,7,8]. It is noteworthy that *Mab* biofilms are particularly tolerant to antibiotics, contributing to their drug resistance [3,6,9]. From smooth strains, rough cord-forming variants could emerge, which are more virulent and cause invasive lung infections [3,6,7].

Current anti-*Mab* therapies rely on old drugs and have very poor success rates [10,11]. One of the reasons is that *Mab* is highly resistant to the currently used antimicrobial drugs [12], and no new antibiotics have been developed specifically for this pathogen [13,14]. Treatment failure leads to an accelerated decline in lung function and, in some countries, *Mab*-infected CF individuals are excluded from lung transplantation lists [3–5]. Recently, kaftrio (elexacaftor/tezacaftor/ivacaftor) was introduced as cystic fibrosis transmembrane conductance regulator (CFTR) gene therapy for selected individuals with CF. Some studies reported that kaftrio treatment can reduce *Mab* infection because it either improves the pathology (less mucus on the lung) or it restores the innate immune function against the pathogen [15,16].

There is, therefore, a crucial need to develop new *Mab*-specific drugs with a novel mechanism of action that is effective against these multi-drug-resistant strains.

The anti-*Mab* drug pipeline is narrowly focused on repurposing or reformulating approved antibiotics for other indications [e.g. bedaquiline, rifabutin, etc. used in tuberculosis (TB) therapy], reminiscent of the dry pipeline scenario in TB research two decades ago [13,14]. However, a few repurposed drugs active against *Mab* have been identified in the last few years, such as the antimalarial OZ439 (targeting DosS-mediated hypoxic signalling), third-generation tetracyclines, the new β-lactam T405, and an epetraborole analogue inhibiting leucyl-tRNA synthetase [17–20]. Furthermore, some new antitubercular compounds have also been shown to be active against *Mab* [21,22]. Recently, activity against *Mab* was shown for the non-drug-like polycationic compound COE-PNH2 [23].

Mab infections are often complicated by co-infections with other pathogens, especially in individuals with CF. A drug inhibiting novel bacterial targets embedded in conserved pathways/functions could therefore be beneficial in such situations.

In recent years, bacterial cell division (CD) has emerged as a critical target in drug discovery [24]. Conserved proteins involved in CD, which often have no counterpart in eukaryotic cells (or low homology), are essential for bacterial survival and have been studied extensively [24,25]. FtsZ is highly conserved due to its essential role in CD [26], and is considered an interesting cellular target for drugs with a broad spectrum of action. FtsZ protein is a structural homolog of the eukaryotic tubulin; both proteins are polymerized in a GTP-dependent manner to form cytoskeletal filaments for CD, but they have different functions [26,27].

FtsZ has been investigated extensively as a potential target of antimycobacterial compounds, and several molecules targeting the *Mtb* enzyme specifically have been reported to act through different mechanisms of action, such as by interference with polymerization or assembly of FtsZ, or inhibiting GTPase activity [28]. Moreover, some FtsZ inhibitors have been identified with anti-*Mab in-vitro* activity [29,30], but have not been further characterized. Thus, despite the high 'druggability' of this enzyme, there are no FtsZ inhibitors in the *Mab* drug development pipeline at present [13].

This study identified a new pyrithione-core molecule, named VOMG, primarily active against *Mab*, but also active against other relevant pathogens including *Mtb* and *Staphylococcus aureus* (*Sau*). Employing a multi-disciplinary approach, this study showed that VOMG displays potent *in-vitro* bactericidal activity against *Mab* in both planktonic and biofilm growth, and in an *in-vivo* mouse model of *Mab* infection. Furthermore, using transcriptomic, biochemical and microbiological approaches, this study showed that VOMG inhibits CD, particularly FtsZ activity.

2. Materials and methods

2.1. High-resolution confocal microscopy for single-cell analysis

Mab ATCC 19977 cells were grown in Middlebrook 7H9 broth at 37°C under shaking conditions (150 rpm) to mid-log phase [optical density at 600 nm (OD_{600}) 0.5–0.8] before snapshot single-cell assay. Fluorescence snapshot imaging was acquired using a 63x glycerol immersion objective installed on an inverted STELLARIS 8 confocal microscope equipped with a 410–850 tunable pulsed white laser. Samples for imaging were prepared bydispensing 0.5 µL of batch culture between two #1.5 coverslips. Exponential-phase *Mab* cells were either treated or not treated with 50 µg/mL of VOMG for 4 and 24 h. To monitor the bacterial changes induced by VOMG treatment accurately, two chemical dyes staining *Mab* chromosome (Hoechst, Frankfurt, Germany) were used to observe possible DNA condensation or the presence of multiple bacterial chromosomes within the same cells, and FM 1-43 (ThermoFisher, Waltham, MA, USA) was used to label mycobacterial membrane. At each mentioned time point, 1 mL of culture was used to perform staining of the bacterial chromosome using Hoescht (1:1000) and the mycobacterial membrane using FM 1-43 (1:1000) for 15 min at room temperature. Next, the stained samples were washed once and resuspended in 50 µL of phosphate buffered saline (PBS). ROI Manager Macro of ImageJ2 (Fiji) 2.9.0/1.53t [31] was used to perform single-cell segmentation. The selection brush tool was used to cover the profile of individual cells, and extract bacterial length and area.

2.2. Biochemical assays with FtsZ proteins

For both *Mab* and *Sau* enzymes, GTPase activity was measured at 30°C, with a spectrophotometric coupled assay using pyruvate kinase and L-lactate dehydrogenase, as described previously [32]. For GTPase inhibition assays, enzymatic activity was determined in the presence of increasing concentrations of VOMG (0.5–100 µM), and the IC_{50} was determined using Equation (1) and GraphPad Prism 9 (GraphPad Software, San Diego, CA, USA):

$$A_{[I]} = A_{[0]} \times \left(1 - \frac{[I]}{[I] + IC_{50}}\right) \quad (1)$$

where $A_{[I]}$ is activity of the enzyme at inhibitor concentration [I]; and $A_{[0]}$ is activity of the enzyme without inhibitor.

The FtsZ inhibitor C109 [29,33] was used as a positive control (data not shown).

The *Sau* FtsZ polymerization assay was performed by sedimentation assay, as described previously [33]. Briefly, the assay was done in 50 mM MES at pH 6.5, 5 mM $Mg(CH_3COO)_2$, 100 mM CH_3CO_2K, 12 µM FtsZ, and 2 mM GTP or GDP. The reaction was incubated at 30°C and 300 rpm for 10 min, and then samples were centrifuged (350,000 × *g*, 10 min, 25°C). The supernatant was immediately separated from the pellet containing the protein polymers, and the samples were analysed by 12% SDS-PAGE with Blue Coomassie staining. The *Mab* FtsZ sedimentation assay was performed as above, but in 50 mM MES at pH 6.5, 5 mM $MgCl_2$ and 50 mM KCl. In both cases, the polymerization assays were conducted in the presence of different concentrations (1–100 µM) of VOMG.

The light scattering assay of FtsZ polymerization was performed as described previously, by measuring the 90° angle light scattering with a Cary Eclipse fluorescence spectrophotometer (Varian, ON, Canada), and using both excitation and emission wavelengths at 400 nm [32]. Polymerization was measured at 30°C in 150 µL of 50 mM MES at pH 6.6, 10 mM $Mg(CH_3COO)_2$ and 100 mM CH_3CO_2K, using FtsZ at a final concentration of 12.5 µM after addition of 1 mM GTP. Data were collected every 5 s.

2.3. In-vivo *efficacy studies of VOMG in mice*

Mice were housed (three to five mice per cage) in the biosafety level 3 animal facility at IRCCS San Raffaele Scientific Institute, Milan, Italy. Lung infection was established to test the efficacy of VOMG *in vivo* using an agar bead C57BL/6 mouse *Mab* infection model [34–36]. Briefly, *Mab* colonies from 7H10 plates were grown for 2 days (to reach exponential phase) in 20 mL of Middlebrook 7H9 broth. For bead preparation, 50 mL of white heavy mineral oil and 25 mL of trypticase soy agar were added to a bacterial suspension, reaching an OD_{600} of 15, and mixed at medium speed with a magnet on a stirrer to generate agar beads, as described previously [37]. Agar bead preparations were stored at 4°C for no more than 1 week; fresh preparations were performed every time. The incorporation of *Mab* in agar beads and the intratracheal injection enabled the bacteria to be physically restrained in the bronchial airways, providing microanaerobic/anaerobic conditions which allow bacteria to grow in microcolonies [34–36]. For the infection, mice were anaesthetized, and the trachea was exposed and intubated. Next, the bead suspension [50 µL, 1×10^5 colony-forming units (CFU)] was injected and the incision was closed with suture clips. Mice intratracheally infected with *Mab* ATCC19977 (1×10^5 CFU) were treated daily with vehicle (saline solution), amikacin (intraperitoneal administration: 100 mg/kg mice, as positive control group) and VOMG by intranasal administration for 7 consecutive days, as described previously [36]. At the end of treatment (8 days post challenge), the mice were euthanized, and their lungs were excised aseptically and homogenized in 2 mL PBS using the homogenizer gentleMACSTM Octo Dissociator. Bacterial loads in local (lung homogenates) and systemic (blood) compartments were determined by plating the samples at 10-fold serial dilution in 7H10 agar medium (Difco; Becton Dickinson, Franklin Lakes, NJ, USA). The experiment was repeated three times.

2.4. Statistical analysis

For biofilm confocal analysis, images were processed with Image J software. Statistical analysis was carried out with Prism 8 (GraphPad Software) using Mann–Whitney test. *P*-values <0.05 were considered to indicate significance.

For single-cell analysis, plots and statistical analysis were generated using Prism 9.4 (GraphPad Software). Welch's *t*-test was performed to compare the variation of a single parameter over multiple groups. *P*-values <0.05 were considered to indicate significance.

Mann–Whitney tests were performed to compare the variation of a single parameter over multiple groups in *in-vivo* experiments. *P*-values <0.05 were considered significant.

3. Results

3.1. Discovery of VOMG as a potent inhibitor of Mab growth

Based on the idea that compounds active against *Mab* sometimes originate from antituberculosis drug discovery campaigns, a range of small-molecule derivatives from the class of pyridine 1-oxides, previously recognized for *in-vitro* activity against *Mtb*, were synthesized [38]. All of these new derivatives were shown to exhibit moderate activity against *Mab* ATCC 19977 growth, with minimal inhibitory concentrations (MICs) ranging from 1 to 2 µg/mL. Structurally, they shared two common structural features: electron-withdrawing groups at position 5 and a carbamimidoylthio fragment (Table S1, see online supplementary material). It was hypothesized that these compounds may act as prodrugs that can be transformed into the same active metabolite that is responsible for their *in-vitro* activity against *Mab*. To confirm this hypothesis, x-VOMG, which is one of the active derivatives, and its two putative degradation products, VOMG and RCB19348, were further studied (Table S1, see online supplementary material; Fig. 1A).

Non-pathogenic *Mycobacterium smegmatis* cultures were incubated in the presence of x-VOMG (MIC = 2.5 µg/mL) and analysed by thin-layer chromatography; x-VOMG was almost completely degraded in the *M. smegmatis* cell extract, and a spot migrating as VOMG base occurred (Fig. 1B,C). Similar results were obtained when both compounds were incubated in 7H9 medium alone, suggesting spontaneous hydrolysis of x-VOMG to VOMG base in aqueous media, as confirmed by mass spectrometry analysis (Fig. 1D–F). These data showed that x-VOMG, and probably all of the pyrithione-based derivatives, are prodrugs converted to the same 5-(ethoxycarbonyl)-2-sulfidopyridine 1-oxide, named VOMG base (the corresponding sodium salt was called VOMG).

VOMG demonstrated higher activity against *Mab* (MIC = 0.125–0.250 µg/mL), whereas RCB19348 was inactive (Fig. 1A; Table S1, see online supplementary material). Structure–activity relationship studies of VOMG revealed that the sulphide substituent is preferable for anti-*Mab* activity compared with the thiocyanate or sulfone substituents. RCB12083 and RCB13031 showed equipotent activity as VOMG, while RCB99063 and RCB12146 displayed diminished activity, and RCB12155 was completely inactive (Table S1, see online supplementary material). Consequently, VOMG was chosen for further studies due to its water-soluble properties, as described in the 'Chemistry' section of the online supplementary material.

3.2. VOMG has bactericidal and antibiofilm activity against Mab, and is suitable for drug combination therapy

Time-kill assays (TKAs) using the reference *Mab* ATCC 19977 strain demonstrated rapid bactericidal activity of VOMG against *Mab* planktonic cells with an early onset of activity (after 24 h) and sterilizing capacity (no regrowth after 14 days of incubation), with a clear concentration cut-off at 1 x MIC value (0.250 µg/mL) (Fig. 2A). This represents an improvement compared with most drugs used in *Mab* therapy that are bacteriostatic [3,13]: amikacin, tigecycline, levofloxacin, imipenem, clofazimine and linezolid also showed a bactericidal effect at the highest concentrations (typically 4 x MIC and 10 x MIC) but with slow onset of activity or no sterilizing capacity (Fig. 2A; Fig. S1, see online supplementary material).

The antibiofilm activity of VOMG was determined following previously described protocols [39] using a high initial inoculum of 10^8 cells/mL to facilitate biofilm formation. Biofilm studies showed a VOMG minimal bactericidal eradication concentration (MBEC) of 128 µg/mL, similar to clarithromycin and amikacin used as positive controls (Fig. 2B). Further studies by confocal laser scanning microscopy showed that biofilm formation was significantly prevented by VOMG (8 µg/mL), similar to clarithromycin, measured as reduction in biofilm thickness and covered surface (Fig. 2C). When a mature biofilm was treated with VOMG (80 µg/mL), the thickness of the mature biofilm was reduced although the covered surface remained constant. Clarithromycin decreased the covered surface of the mature biofilm but had no effect on biofilm thickness, while amikacin had no activity against *Mab* biofilms. The three

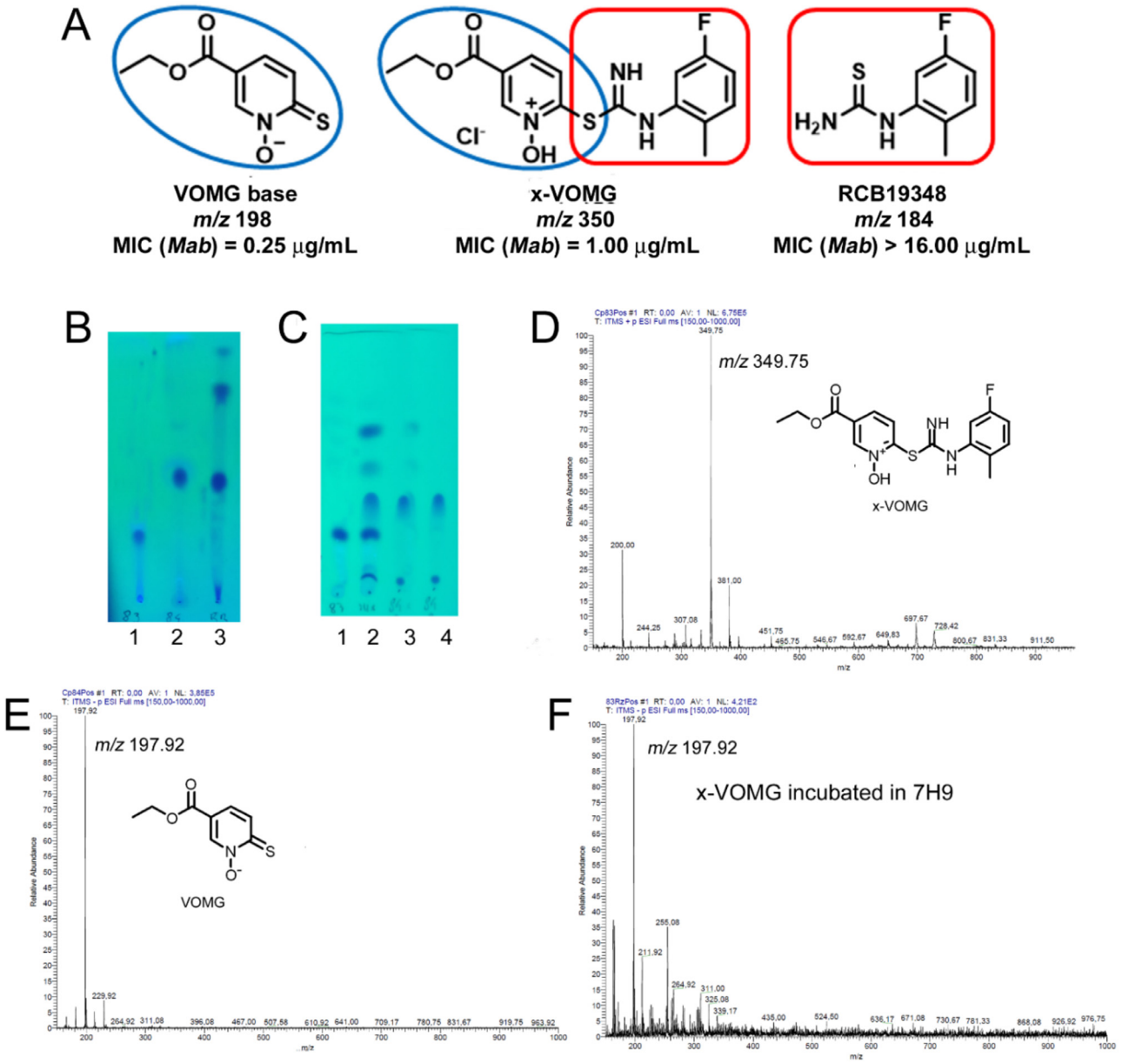

Fig. 1. Discovery of VOMG as the active metabolite of x-VOMG. (A) Transformation of x-VOMG into its metabolites, including VOMG. (B) Thin-layer chromatography (TLC) analysis of the extracts of *Mycobacterium smegmatis* cultures treated with: (1) x-VOMG; (2) VOMG; and (3) extract of culture treated with x-VOMG. (C) TLC analysis of the compounds after 24 h of incubation in 7H9 medium: (1) x-VOMG; (2) x-VOMG extracted after incubation in 7H9; (3) VOMG extracted after incubation in 7H9; and (4) VOMG. (D) Mass spectrometry analysis of x-VOMG. (E) Mass spectrometry analysis of VOMG. (F) Mass spectrometry analysis of x-VOMG extracted after incubation in 7H9 medium.

compounds had a reduced effect against the mature biofilm at a lower concentration (8 μg/mL) (Fig. S2, see online supplementary material).

The potential inclusion of VOMG in combinational *Mab* therapy was evaluated by combinatorial TKA assay with nine currently used anti-*Mab* compounds. No antagonism was identified, indicating the suitability of VOMG for combination therapy (Fig. S3, see online supplementary material).

3.3. VOMG displays broad-spectrum antibacterial activity and is active against drug-resistant clinical isolates

The water-soluble VOMG molecule (Table S1, see online supplementary material) showed greater activity than its prodrug x-VOMG against all the mycobacterial species tested, including *Mab, Mycobacterium avium* and *Mtb* drug-resistant isolates (Table S2, see online supplementary material). VOMG was also active against *Escherichia coli, Acinetobacter baumannii* and *Sau,* including methicillin-resistant clinical isolates (Table S3, see online supplementary material), while it was inactive against *Klebsiella pneumoniae* and *Pseudomonas aeruginosa* (MIC >128 μg/mL). However, activity against *P. aeruginosa* could be restored in the presence of the efflux pump inhibitor PaβN (MIC = 1 μg/mL). VOMG was also active against some fungal species (Table S4, see online supplementary material).

3.4. VOMG has favourable ADME-Tox profile and shows efficacy in a mouse model of Mab infection

VOMG revealed good metabolic stability in mouse and human liver microsomes, low levels of CYP inhibition, no mutagenicity

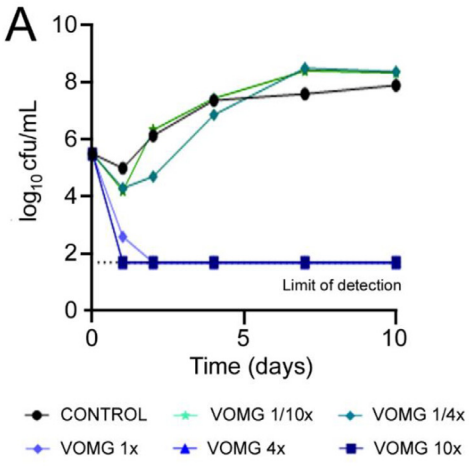

B

Compounds	Activity against *Mab* ATCC 19977 (μg/mL) MIC	MBEC
x-VOMG	1.00	256.00
VOMG	0.25	128.25
Clarithromycin	4.00	128.00
Amikacin	32.00	64.00

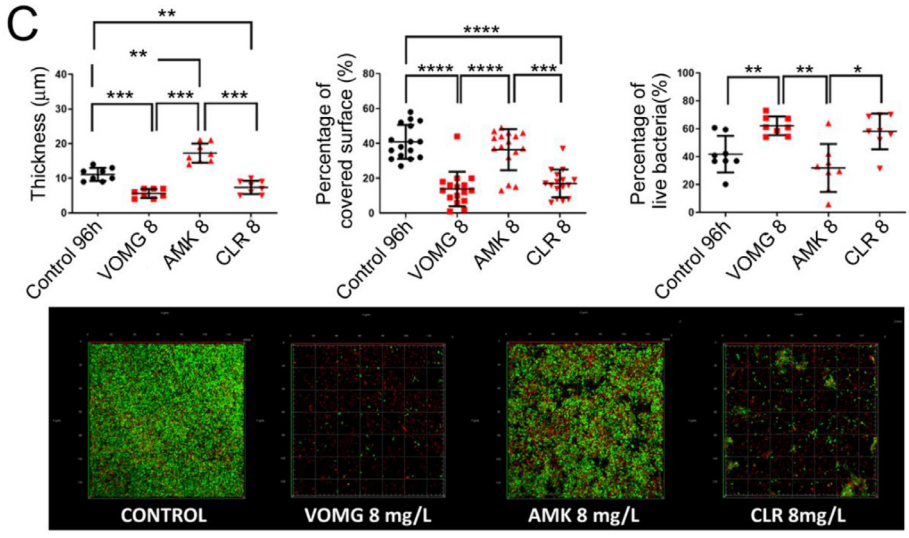

Fig. 2. VOMG has bactericidal and antibiofilm activity against *Mycobacterium abscessus* (*Mab*). (A) Time-kill assay of VOMG in *Mab*. The graph is representative of three different experiments (each experiment includes two technical replicates). (B) Minimum inhibitory concentration (MIC) and minimum biofilm eradication concentration (MBEC) of VOMG and x-VOMG against *Mab*. (C) Prevention of biofilm formation with VOMG, clarithromycin and amikacin at 8 μg/mL.

(Ames fluctuation test) and no cardiotoxicity (hERG assay) signals (Table S5, see online supplementary material).

A chronic toxicity study in healthy C57BL/6 male mice following a single oral administration of VOMG (50 mg/kg) showed no adverse effects during the 2-week observation period (Table S6, see online supplementary material). The acute toxicity study in mice showed a LD_{50} of 455.78 ± 21.79 mg/kg.

Pharmacokinetics studies in mice revealed good bioavailability of VOMG. Peak plasma concentrations were achieved after 4 h following a single oral administration. VOMG was eliminated gradually, with a mean retention time of 18.3 h and a half-life of 12.3 h. The apparent volume of distribution was established as 273.6 mL/g, and apparent total body clearance was 15.38 mL/h/g (Fig. 3A; Table S7, see online supplementary material).

The *in-vivo* efficacy of VOMG was tested using different doses (50, 100 and 500 mg/kg bw) in C57BL/6NCrl mice infected with agar-embedded *Mab* cells. Intranasal administration of VOMG at the lowest dose tested (50 mg/kg body weight) significantly reduced the bacterial load in the lungs and at systemic levels in blood samples in comparison with the control untreated infected groups. The results were comparable to those observed in the positive control group treated with amikacin (Fig. 3B–D).

3.5. VOMG and its prodrug inhibit CD

To study the mechanism of action of VOMG, first the authors tried to generate *in-vitro* VOMG-resistant mutants in *Mab, Mtb* and *M. smegmatis* using a strain lacking NucS/EndoMS [40]. All attempts were unsuccessful, suggesting a cellular target essential for mycobacterial cell growth. Next, the authors screened a panel of *Mtb* mutants resistant to known drugs, which harbour identified mutations in genes encoding targets [41–44], activators [43,45] and associated mechanisms of drug resistance [43,46,47]; these strains were all sensitive to VOMG (Table S8, see online supplementary material), suggesting a different mechanism of resistance from those represented in the panel.

Finally, *Mab* cultures treated with x-VOMG (10- and 20-fold MIC, plus untreated controls) were subjected to transcriptomics to identify differentially expressed genes (DGEs). In total, 493 genes were found to be differentially expressed in both treatments compared with controls: 363 upregulated and 130 downregulated (Table S9, see online supplementary material) (Fig. 4A–C). The level of expression of three DGEs (two induced and one repressed) was also confirmed by quantitative real-time polymerase chain reaction (Table S10, see online supplementary material). Assignment of *Mab*

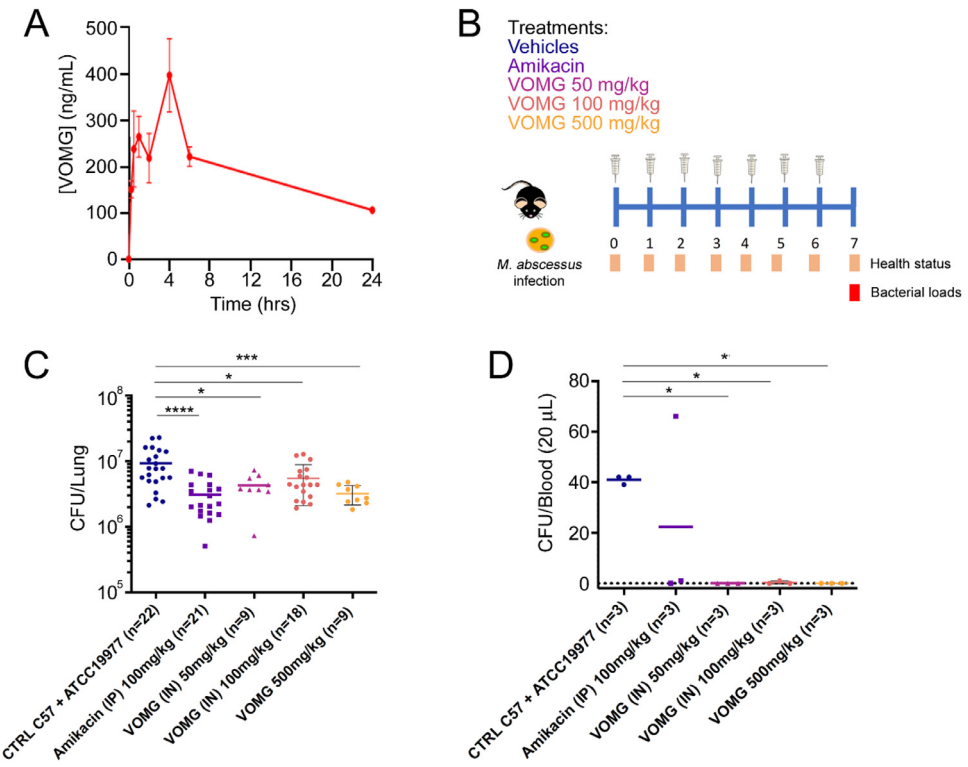

Fig. 3. VOMG has good bioavailability and is effective *in vivo*. (A) Pharmacokinetics of VOMG after 100 mg/kg *per os* administration in mice. (B) Evaluation of the efficacy of VOMG (50, 100 and 500 mg/kg) in immunocompetent C57BL/6NCrl mice infected with agar-embedded *Mycobacterium abscessus* cells by intranasal administration. Amikacin (100 mg/kg, IP) was used as internal control. Timeline of the experiment. (C) VOMG at 50, 100 and 500 mg/kg reduced the bacterial burden in the lungs significantly compared with infected groups. (D) A similar trend in bacterial burden reduction after VOMG treatment was observed in blood samples. CFU, colony-forming unit.

ATCC 19977 genes to functional categories revealed that most DGEs fall within seven functional categories [48]. The most represented groups were 'conserved hypothetical proteins' and 'intermediary metabolism and respiration' (Fig. 4C).

The most overexpressed genes were associated with compound-induced stress, such as genes encoding catalase, carbonic anhydrase (*MAB_3211c*), kinase, and alternative sigma factors [49]. Interestingly, overexpression of several genes encoding proteins involved in metal metabolism (e.g. ArsR, ArsC, etc.), nitrogen and sulphur metabolism, and membrane proteins (e.g. efflux pumps, chaperonines and heat shock proteins) was observed (Fig. 4C). These data suggested that x-VOMG treatment could cause cellular stress, affecting cell permeability and disrupting metal homeostasis.

Genes involved in transcription, protein and ATP synthesis processes were shut-down by x-VOMG treatment (genes encoding RNA polymerase subunits such as *rpoB*; RHO factor and NusG factor; ribosomal proteins such as *rpmI, rpmT, rpmD*; translation initiation factors; operon coding for ATP synthase) [50,51]. Cellular respiration was also inhibited (e.g. genes encoding quinones and cytochromes), as well as genes encoding MCE proteins, promoting macrophage invasion [52]. Interestingly, the most downregulated operon was the highly conserved division cell wall (*dcw*) operon essential for *Mab* growth. Genes coding for FtsZ, FtsQ, SepF (positive CD regulator), SteA and SteB (involved in the last CD steps), and MurC and MurG (involved in peptidoglycan biosynthesis) were downregulated (Table S11, see online supplementary material).

These findings suggest that x-VOMG, and consequently its active metabolite VOMG, could inhibit CD, particularly FtsZ.

The morphological *Mab* single-cell changes (i.e. area and length) induced by VOMG (50 µg/mL, 200 x MIC) after 4 and 24 h of treatment were monitored (Fig. 4D,E). Single-cell analysis revealed that, particularly after 24 h of VOMG treatment, *Mab* cells exhibited a significant increase in both bacterial area and length compared with the untreated control (Fig. 4D,E). In addition, the bacterial septum (white arrow in Fig. 4D) could be observed in the cells treated with VOMG for 4 h, together with multiple condensation foci, conformation putatively compatible with the presence of multiple copies of the chromosome [53], suggesting an interruption in mycobacterial replication (Fig. 4D). Similarly, aberrant elongation, increased area and multiple chromosome foci within the same cell were observed in the 24-h-treated cells (Fig. 4E). These results confirm the RNA-seq findings indicating that VOMG dysregulates *Mab* CD.

3.6. VOMG inhibits FtsZ activity not only in Mab but also in Sau through different mechanisms

Mab and *Sau* [33] FtsZ proteins were produced recombinantly (Fig. S4, see online supplementary material), and the ability of VOMG to directly inhibit FtsZ GTPase activity and its ability to form polymers was evaluated. VOMG was able to block FtsZ GTPase activity, but displayed only weak effects (IC_{50} values of 54.0 ± 3.6 µM and 18.5 ± 1.8 µM for *Mab* and *Sau* FtsZ, respectively) (Fig. 5A,B). Thus, it was tested whether VOMG could interfere directly with FtsZ polymerization. An *in-vitro* sedimentation assay demonstrated that VOMG inhibited the formation of *Mab* FtsZ polymers in a concentration-dependent manner (Fig. 5C). This was in contrast to the effect observed against *Sau* FtsZ, where the quantity of the polymerized protein increased (Fig. 5D), suggesting that the effect of VOMG on FtsZ polymerization differs in the two pathogens. So, while VOMG inhibited polymer formation in *Mab*, it modified polymerization kinetics in *Sau*, increasing the quantity of polymers formed or affecting their stability.

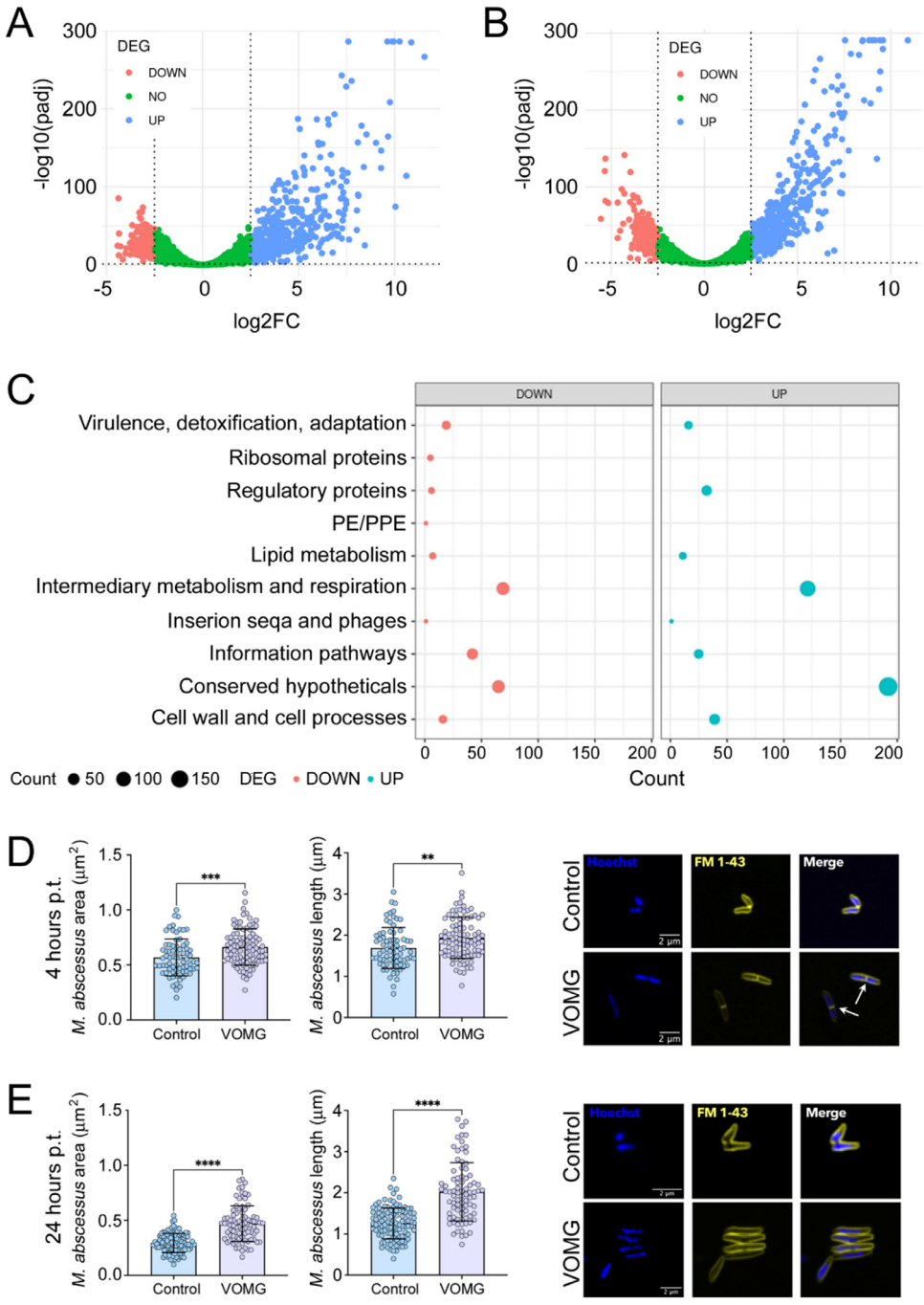

Fig. 4. x-VOMG inhibits several key metabolic pathways, in particular cell division. (A) Volcano plot showing *Mycobacterium abscessus* (*Mab*) genes up- (blue) and down-regulated (red) in response to x-VOMG treatment (10 µg/mL). (B) Volcano plot showing *Mab* genes up- (blue) and downregulated (red) in response to x-VOMG treatment (20 µg/mL). (C) COG enrichment plot showing shared categories significantly down- (red) and upregulated (blue) in response to x-VOMG treatment. (D) Single-cell area and length of *Mab* wild-type strain treated with 50 µg/mL of VOMG or not for 4 h. On the right, representative snapshot images of *Mab* wild-type strain treated with 50 µg/mL of VOMG or not (control) for 4 h and stained with Hoechst and FM 1-43. (E) Single-cell area and length of *Mab* wild-type strain treated with 50 µg/mL of VOMG or not for 24 h. Black lines indicate mean ± SD ($83 > n < 103$). On the right, representative snapshot images of *Mab* wild-type strain treated with 50 µg/mL of VOMG or not (control) for 24 h and stained with Hoechst and FM 1-43. Asterisks denote significant difference by Welch's *t*-test: $^{**}P = 0.0021$; $^{***}P = 0.0004$; $^{****}P < 0.0001$. Hoechst (blue) and FM 1-43 (yellow) are shown separately and merged, as indicated in the snapshots. Scale bar 2 µm.

This evidence was confirmed by FtsZ polymerization kinetic studies through 90° light scattering assays. In *Mab*, VOMG initially induced very rapid FtsZ polymerization, probably leading to unstable polymers that collapsed rapidly. The protein was no longer able to form polymers at the highest concentrations (Fig. 5E). In contrast, in *Sau*, FtsZ polymerized faster, but the depolymerization rate decreased; consequently, polymer disassembly was longer than in the untreated control (Fig. 5F). These data confirmed that FtsZ polymer assembly and, consequently, bacterial CD were dramatically impacted by VOMG in both species.

4. Discussion

Over the last 15 years, *Mab* has emerged as a worrying pathogen causing several clinical manifestations, particularly lung infections in individuals suffering from CF and COPD. In these pop-

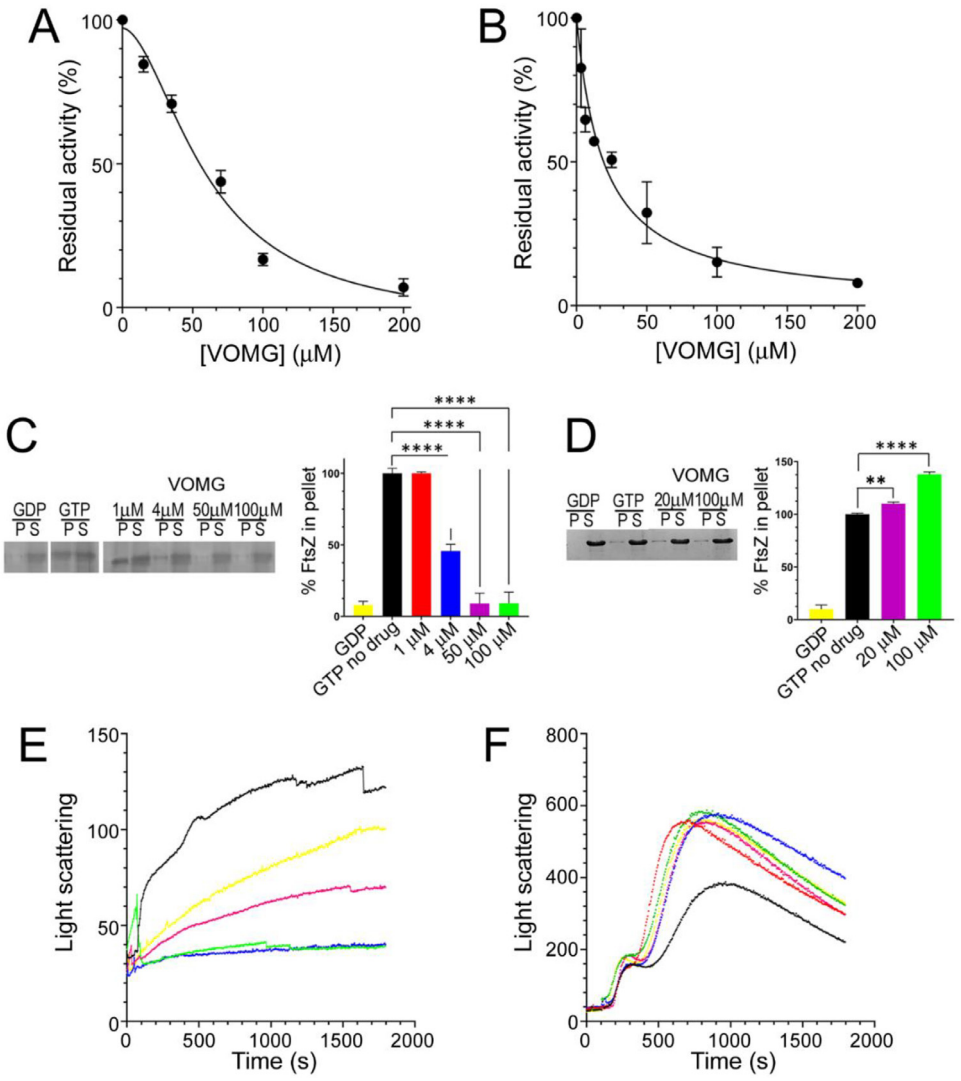

Fig. 5. VOMG inhibits FtsZ activity in both *Mycobacterium abscessus* (*Mab*) and *Staphylococcus aureus* (*Sau*). (A) IC_{50} determination of VOMG against *Mab* FtsZ GTPase activity. Data are mean ± SD from three different replicates. (B) IC_{50} determination of VOMG against *Sau* FtsZ GTPase activity. Data are mean ± SD from three different replicates. (C) SDS-PAGE of sedimentation assay of *Mab* FtsZ in the presence/absence of VOMG. (D) SDS-PAGE of sedimentation assay of *Sau* FtsZ in the presence/absence of VOMG. P, insoluble fraction (pellet); S, soluble fraction (supernatant). Images are representative of at least three different experiments. On the right, the densitometric analysis of the gels is reported; the density of the protein band in the pellet of the reactions performed with GTP in the absence of VOMG was used as reference and considered as 100% ($^{**}P < 0.01$, $^{****}P < 0.0001$ one-way analysis of variance). (E) Light scattering polymerization assay of *Mab* FtsZ in the absence (black line) or presence of increasing concentration of VOMG (400 μM, red line; 200 μM, blue line; 100 μM green line; 50 μM, purple line, 25 μM, yellow line). (F) Light scattering polymerization assay of *Sau* FtsZ in the absence (black line) or presence of increasing concentration of VOMG (as in E).

ulations, *Mab* infection treatment outcomes are usually poor [3–5]. Unfortunately, the elevated rates of attrition in the drug development process are linked directly to the limited options available in the anti-*Mab* drug pipeline. In fact, currently recommended and available therapeutic strategies are mainly based on repositioning antibiotics used for other indications, such as TB, and there are no specific new drugs on the horizon that can prevent *Mab* from becoming the next superbug [13,14]. Innovative approaches such as phage therapy can represent alternative therapies, although their wide clinical implementation remains a challenge, leaving options for personalized medicine [54].

VOMG was discovered in a focused screening to identify novel compounds active against *Mab* (one compound active against *Mab* growth out of more than 700 tested; M.R. Pasca, V. Makarov, personal communication). VOMG is a highly polar molecule that has positive and negative centres, as well as hydrophilic and lipophilic moieties in its structure. For these reasons, it can easily cross mycobacterial cell walls, like isoniazid. Furthermore, like drugs targeting enzymes located inside the cell, VOMG has hydrophilic moieties. Lipophilicity may be a key factor for antitubercular agents that target enzymes in the cell membrane [55,56]. VOMG fully complies with Lipinski's rules (less than five donor hydrogen bonds; <10 acceptor hydrogen bonds; molecular weight <500; octanol–water distribution coefficient <5).

VOMG is a pyrithione-core small molecule (x-VOMG is its prodrug) with a strong substituent at position 5 of the ring that withdraws electrons from sulphur and makes any chelation of metals other than copper unattainable (according to the Irving–Williams series of metal complex stability). Many drugs in the market can chelate copper and, very often, it corresponds to their toxicity-related mechanism of action towards bacterial cells [57,58]. In the case of VOMG, its preliminary safety profile was demonstrated through various assays, including *in-vitro* and *in-vivo* studies such as ADME-Tox assays, and acute and subchronic toxicity studies in mice. In fact, pharmacokinetic and toxicity studies using an oral dose of 100 mg/kg body weight showed no toxicity and high safety

(mean Cmax value 400 ng/mL, which is above the MIC value of 250 ng/mL). ADME studies confirm the lack of toxicity signals in VOMG. In the *in-vivo* studies, intranasal delivery directly into the lungs may have further increased concentration values directly at the site of infection, reducing systemic toxicity. Finally, VOMG could be suitable for novel drug delivery formulations, including aerosol inhalation [59], owing to its favourable physicochemical properties, such as water solubility, good oral bioavailability, and absence of toxicity [60].

The average success rate of *Mab* drug therapy is approximately 45% [61], as most drugs used as anti-*Mab* therapeutics are bacteriostatic [3,62], they have no antibiofilm activity, and they are ineffective against drug-resistant isolates of this pathogen. In contrast, VOMG exhibits high bactericidal activity *in vitro*, eradicating *Mab* in planktonic culture, and antibiofilm properties. It is also active against drug-resistant *Mab* clinical isolates, including multi-drug-resistant strains. TKAs showed a clear concentration cut-off with lack of dose range correlation with activity. At a concentration of just 1 x MIC (0.25 µg/mL), VOMG reduced the bacterial load rapidly and cleared the culture. This activity was more potent than that of the currently recommended clarithromycin and amikacin, or of other drugs under development [63]. VOMG was also equally or more active than the standard of care drugs against *Mab* biofilm. Indeed, only a few compounds are active against *Mab* biofilm, such as clarithromycin, which was used in this study as the control [64]. The antibiofilm activity was observed using two complementary approaches: prevention of biofilm formation and treatment of a mature biofilm. VOMG is also active against drug-resistant *Mab* clinical isolates, including multi-drug-resistant strains. Furthermore, the authors were unable to isolate mutants resistant to VOMG *in vitro*, which is a key aspect for infectious drug development, and is one of the most advantageous features of VOMG.

The bactericidal and eradicating properties of VOMG, together with its broad-spectrum antimicrobial activity and antibiofilm properties, strongly reinforce the potential of VOMG for the treatment of pulmonary infections, especially in individuals with CF, even when the standard of care treatment is not effective.

A significant roadblock in the development of novel drugs against *Mab* is the absence of a validated mouse model of chronic *Mab* pulmonary disease suitable for evaluating the *in-vivo* efficacy of novel therapeutics. BALB/c mice infected intranasally with a high dose produced an infection that progressed to approximately 10^7 CFU/mL in the lungs after14 days post infection [63]. C3HeB/FeJ mice aerosol-infected and treated with corticosteroids showed progression of the infection, reaching moderate bacterial burdens (approximately 4–5 log10 CFU/mL in the lungs), but allowing for extended 4-week treatment schedules [65,20]. The present study used an alternative C57BL/6 model of *Mab* infection embedded within agar beads and delivered directly to the bronchial airways providing microanaerobic/anaerobic conditions that allow bacteria to grow in microcolonies [34–36], more accurately resembling the natural lung environment in CF individuals. In this model, a 7-day intranasal treatment of VOMG was able to contain the bacterial burden in the lungs and blood similar to the effect achieved with amikacin (used as control), which was administered intraperitoneally. VOMG water solubility, coupled with the *in-vivo* findings by intranasal administration, could allow speculation on the possibility for nebulization delivery. Similar to what was observed in the TKA studies, there was no dose proportionality in the effect of the treatment; i.e. no significant differences were observed between the lowest dose (50 mg/kg body weight) and the highest dose (500 mg/kg body weight), suggesting that the lowest efficacious dose has not yet been defined, and that once an effective dose has been reached, further increase may not be needed.

The mode of action of VOMG is novel; transcriptional analysis revealed inhibition of key metabolic pathways, such as CD, protein synthesis, ATP production and gene transcription. Genes encoding FtsZ and other CD proteins are the most downregulated in the presence of VOMG, pointing out possible inhibition of FtsZ. Single-cell analysis and biochemical assays confirmed that VOMG affects the organization of FtsZ polymers and, consequently, CD.

FtsZ is highly conserved among micro-organisms [26], which is consistent with the broad-spectrum activity observed for VOMG. The mechanism of action of VOMG seems to be very peculiar as it is not only able to block FtsZ GTPase activity, but also to modify the polymerization kinetics of the protein which, overall, reflect an alteration of *in-vivo* CD organization and assembly rate.

VOMG has a distinct impact on the polymerization of *Mab* and *Sau* FtsZ proteins. This could be due to the low identity percentage of the C-terminal region of the two proteins implicated in protofilament formation and in lateral interactions of polymers [66]. Interestingly, the FtsZ inhibitor PC190723, which is active against *Sau* and *Bacillus subtilis*, has been reported to induce polymer stabilization and suppress *in-vivo* FtsZ polymer dynamics [67], similar to the effect of VOMG on *Sau* FtsZ.

VOMG also increases the rate at which *Mab* FtsZ polymerizes for a short time and then decreases it. This feature could be beneficial in a multi-drug regimen. VOMG could increase the polymerization rate, leading to an increased extracellular growth rate, becoming more sensitive to VOMG and other co-administered drugs targeting actively growing bacteria.

Although several FtsZ inhibitors have been identified in recent years [29,30], none of them are currently under development as anti-*Mab* compounds at any stage of the process.

In conclusion, VOMG is a new water-soluble compound targeting *Mab* specifically with good *in-vitro*, *in-vivo* and ADME/Tox properties, and a novel mode of action specific for bacteria, inhibiting CD. These features bring promise for a new drug candidate with the possibility to use different formulations in the much needed and narrow *Mab* drug development pipeline. Potential progression of VOMG into the clinic might bring new therapeutic options to treat lung disease caused by this pathogen and other susceptible microorganisms.

Funding: This work was supported by: Italian Cystic Fibrosis Research Foundation grants: FFC#19/2018 (adopted by Delegazione FFC di Brindisi Torre, Delegazione FFC di Ascoli Piceno, Delegazione FFC di Novara) (MRP); FFC#14/2020 (adopted by Smartform/Tattooform, Delegazione FFC di Belluno con i rocciatori di Fonzaso) (MRP, VM, SRG, ET); FFC#18/2021 (adopted by Delegazione FFC Ricerca di Codogno e Piacenza, Delegazione FFC Ricerca di Rovigo, Delegazione FFC Ricerca di Belluno, Nonno Nanni Latteria Montello) (MRP, VM, SRG, ET); and FFC#09/2023 (adopted by Carolina Sabatini, Delegazione FFC Ricerca di Siniscola Nuoro, Gruppo di sostegno FFC Ricerca di Casale Monferrato, Delegazione FFC Ricerca della Valdadige, Delegazione FFC Ricerca di Crevalcore) (MRP, FS). This work was partially supported by NextGenerationEU-MUR PNRR Extended Partnership Initiative on Emerging Infectious Diseases (Project No. PE00000007, INF-ACT) (MRP). LM-M was supported by a fellowship from the Government of Aragon (Gobierno de Aragón y Fondos FEDER de la Unión Europea 'Construyendo Europa desde Aragón'). JME-A was funded by a fellowship from the Spanish Government (Programa de Formación de Profesorado Universitario, Ref. FPU18/03873).

Competing Interests: GD, OR, VM and MRP have filed a patent related to this work (P2245IT, PCT/EP2023/078712). The other authors declare no competing interests.

Ethical approval: Animal work for the evaluation of pharmacokinetics and toxicity was performed under protocols approved by the Animal Care and Use Committee of the Research Centre of Biotechnology RAS (Moscow, Russia) according to the centre's guide-

lines for animal use; the state industry standards GOST 33044-2014, GOST 33215-2014 and GOST 33216-2014; European Directive 2010/63/EC for animal experiments; and Guide for the Care and Use of Laboratory Animals. 8th edition (Washington, DC: National Academies Press; 2011). Animal studies for in-vivo infection were conducted according to protocols in strict adherence to the Italian Ministry of Health guidelines for the use and care of experimental animals (Ref. No. 1242), and approved by the San Raffaele Scientific Institute Institutional Animal Care and Use Committee.

Sequence information: The RNA-seq data have been deposited in the NCBI Sequence Read Archive database under BioProject accession number SUB13481799 (BioSample accessions: SAMN35540038, SAMN35540039, SAMN35540040, SAMN35540041, SAMN35540042, SAMN35540043, SAMN35540044, SAMN35540045, SAMN35540046).

Acknowledgments

The authors wish to thank Stewart Cole (Pasteur Institute, Paris, France) and Claudia Sala (Fondazione Toscana Life Sciences, Siena, Italy) for providing NTM strains and *M. abscessus* multi-drug-resistant clinical isolate n. 1. The authors also wish to thank Dr. Ersilia V. Fiscarelli (Ospedale Pediatrico Bambino Gesù, Rome, Italy) and Dr. Lanfranco Fattorini (ISS, Rome, Italy) for providing *M. abscessus* multi-drug-resistant clinical isolate n. 2 and NTM drug-resistant clinical isolates, respectively. Finally, the authors wish to thank Dr. Anna Egorova (Federal Research Centre 'Fundamentals of Biotechnology' of the Russian Academy of Sciences, Russia) for the fruitful discussion during the drafting of the manuscript.

Supplementary materials

Supplementary material associated with this article can be found, in the online version, at doi:10.1016/j.ijantimicag.2024.107278.

References

[1] Boudehen Y, Kremer L. Microbe of the month: Mycobacterium abscessus. Trends Microbiol 2021;29:951–2.
[2] Bryant JM, Brown KP, Burbaud S, Everall I, Belardinelli JM, Rodriguez-Rincon D, et al. Stepwise pathogenic evolution of Mycobacterium abscessus. Science 2021;372:eabb8699.
[3] Degiacomi G, Sammartino JC, Chiarelli LR, Riabova O, Makarov V, Pasca MR. Mycobacterium abscessus, an emerging and worrisome pathogen among cystic fibrosis patients. Int J Mol Sci 2019;20:5868.
[4] Johansen MD, Herrmann JL, Kremer L. Non-tuberculous mycobacteria and the rise of Mycobacterium abscessus. Nat Rev Microbiol 2020;18:392–407.
[5] Martiniano SL, Nick JA, Daley CL. Nontuberculous mycobacterial infections in cystic fibrosis. Clin Chest Med 2022;43:697–716.
[6] Nguyen TQ, Heo BE, Jeon S, Ash A, Lee H, Moon C, Jang J. Exploring antibiotic resistance mechanisms in Mycobacterium abscessus for enhanced therapeutic approaches. Front Microbiol 2024;15:1331508.
[7] Ciofu O, Tolker-Nielsen T, Jensen PØ, Wang H, Høiby N. Antimicrobial resistance, respiratory tract infections and role of biofilms in lung infections in cystic fibrosis patients. Adv Drug Deliv Rev 2015;85:7–23.
[8] Uruén C, Chopo-Escuin G, Tommassen J, Mainar-Jaime RC, Arenas J. Biofilms as promoters of bacterial antibiotic resistance and tolerance. Antibiotics 2020;10:3.
[9] Nasrollahian S, Pourmoshtagh H, Sabour S, Hadi N, Azimi T, Soleiman-Meigooni S. Biofilm formation in mycobacterial genus; mechanism of biofilm formation and anti-mycobacterial biofilm agents. Curr Pharm Biotechnol 2024 Online ahead of print. doi:10.2174/0113892010277107240227054933.
[10] Daley CL, Iaccarino JM, Lange C, Cambau E, Wallace RJ Jr, Andrejak C, et al. Treatment of nontuberculous mycobacterial pulmonary disease: an official ATS/ERS/ESCMID/IDSA clinical practice guideline. Clin Infect Dis 2020;71:e1–36.
[11] Fröberg G, Maurer FP, Chryssanthou E, Fernström L, Benmansour H, Boarbi S, et al. EUCAST AMST and ESCMYC study groups. Towards clinical breakpoints for non-tuberculous mycobacteria – determination of epidemiological cut off values for the Mycobacterium avium complex and Mycobacterium abscessus using broth microdilution. Clin Microbiol Infect 2023;29:758–64.
[12] Luthra S, Rominski A, Sander P. The role of antibiotic-target-modifying and antibiotic-modifying enzymes in Mycobacterium abscessus drug resistance. Front Microbiol 2018;9:2179.
[13] Egorova A, Jackson M, Gavrilyuk V, Makarov V. Pipeline of anti-Mycobacterium abscessus small molecules: repurposable drugs and promising novel chemical entities. Med Res Rev 2021;41:2350–87.
[14] Tunesi S, Zelazny A, Awad Z, Mougari F, Buyck JM, Cambau E. Antimicrobial susceptibility of Mycobacterium abscessus and treatment of pulmonary and extra-pulmonary infections. Clin Microbiol Infect 2024;30:718–25.
[15] Wiesel V, Aviram M, Mei-Zahav M, Dotan M, Prais D, Cohen-Cymberknoh M, et al. Eradication of nontuberculous mycobacteria in people with cystic fibrosis treated with elexacaftor/tezacaftor/ivacaftor: a multicenter cohort study. J Cyst Fibros 2024;23:41–9.
[16] Gavey R, Nolan J, Moore V, Reid D, Brown J. Clinical and radiological improvement of cavitary Mycobacteroides abscessus disease in cystic fibrosis following initiation of elexacaftor/tezacaftor/ivacaftor. J Cyst Fibros 2024;21 S1569-1993(24)00071-7Online ahead of print. doi:10.1016/j.jcf.2024.05.008.
[17] Belardinelli JM, Verma D, Li W, Avanzi C, Wiersma CJ, Williams JT, et al. Therapeutic efficacy of antimalarial drugs targeting DosRS signaling in Mycobacterium abscessus. Sci Transl Med 2022;14:eabj3860.
[18] Li A, He S, Li J, Zhang Z, Li B, Chu H. Omadacycline, eravacycline, and tigecycline express anti-Mycobacterium abscessus activity in vitro. Microbiol Spectr 2023;4:e0071823.
[19] Nguyen TQ, Heo BE, Hanh BTB, Jeon S, Park Y, Choudhary A, et al. DS86760016, a leucyl-tRNA synthetase inhibitor, is active against Mycobacterium abscessus. Antimicrob Agents Chemother 2023;22:e0156722.
[20] Rimal B, Batchelder HR, Story-Roller E, Panthi CM, Tabor C, Nuermberger EL, et al. T405, a new penem, exhibits in vivo efficacy against M. abscessus and synergy with β-lactams imipenem and cefditoren. Antimicrob Agents Chemother 2022;66:e0053622.
[21] Negatu DA, Beuchel A, Madani A, Alvarez N, Chen C, Aragaw WW, et al. Piperidine-4-carboxamides target DNA gyrase in Mycobacterium abscessus. Antimicrob Agents Chemother 2021;65:e0067621.
[22] Lang M, Ganapathy US, Mann L, Abdelaziz R, Seidel RW, Goddard R, et al. Synthesis and characterization of phenylalanine amides active against Mycobacterium abscessus and other mycobacteria. J Med Chem 2023;66:5079–98.
[23] Zhang K, Limwongyut J, Moreland AS, Wei SCJ, Jim Jia Min T, Sun Y, et al. An anti-mycobacterial conjugated oligoelectrolyte effective against Mycobacterium abscessus. Sci Transl Med 2024;16:eadi7558.
[24] den Blaauwen T, Andreu JM, Monasterio O. Bacterial cell division proteins as antibiotic targets. Bioorg Chem 2014;55:27–38.
[25] Donovan C, Bramkamp M. Cell division in Corynebacterineae. Front Microbiol 2014;5:132.
[26] Pradhan P, Margolin W, Beuria TK. Targeting the Achilles heel of FtsZ: the interdomain cleft. Front Microbiol 2021;12:732796.
[27] Han H, Wang Z, Li T, Teng D, Mao R, Hao Y, et al. Recent progress of bacterial FtsZ inhibitors with a focus on peptides. FEBS J 2021;288:1091–106.
[28] Shinde Y, Pathan A, Chinnam S, Rathod G, Patil B, Dhangar M, et al. Mycobacterial FtsZ and inhibitors: a promising target for the anti-tubercular drug development. Mol Divers 2023 Online ahead of print. doi:10.1007/s11030-023-10759-8.
[29] Hogan AM, Scoffone VC, Makarov V, Gislason AS, Tesfu H, Stietz MS, et al. Competitive fitness of essential gene knockdowns reveals a broad-spectrum antibacterial inhibitor of the cell division protein FtsZ. Antimicrob Agents Chemother 2018;62 e01231-18.
[30] Low JL, Wu ML, Aziz DB, Laleu B, Dick T. Screening of TB Actives for activity against nontuberculous mycobacteria delivers high hit rates. Front Microbiol 2017;8:1539.
[31] Schneider CA, Rasband WS, Eliceiri KW. NIH Image to ImageJ: 25 years of image analysis. Nat Methods 2012;9:671–5.
[32] Król E, Scheffers DJ. FtsZ polymerization assays: simple protocols and considerations. J Vis Exp 2013;81:e50844.
[33] Trespidi G, Scoffone VC, Barbieri G, Marchesini F, Abualsha'ar A, Coenye T, et al. Antistaphylococcal activity of the FtsZ inhibitor C109. Pathogens 2021;10:886.
[34] Saliu F, Rizzo G, Bragonzi A, Cariani L, Cirillo DM, Colombo C, et al. Chronic infection by nontypeable Haemophilus influenzae fuels airway inflammation. ERJ Open Res 2021;7:00614–2020.
[35] Lorè NI, Saliu F, Spitaleri A, Schäfle D, Nicola F, Cirillo DM, Sander P. The aminoglycoside-modifying enzyme Eis2 represents a new potential in vivo target for reducing antimicrobial drug resistance in Mycobacterium abscessus complex. Eur Respir J 2022;60:2201541.
[36] Nicola F, Cirillo DM, Lorè NI. Preclinical murine models to study lung infection with Mycobacterium abscessus complex. Tuberculosis 2023;138:102301.
[37] Riva C, Tortoli E, Cugnata F, Sanvito F, Esposito A, Rossi M, et al. A new model of chronic Mycobacterium abscessus lung infection in immunocompetent mice. Int J Mol Sci 2020;21:6590.
[38] Salina EG, Ryabova O, Vocat A, Nikonenko B, Cole ST, Makarov V. New 1-hydroxy-2-thiopyridine derivatives active against both replicating and dormant Mycobacterium tuberculosis. J Infect Chemother 2017;23:794–7.
[39] Muñoz-Egea MC, García-Pedrazuela M, Mahillo I, Esteban J. Effect of ciprofloxacin in the ultrastructure and development of biofilms formed by rapidly growing mycobacteria. BMC Microbiol 2015;15:18.
[40] Castañeda-García A, Prieto AI, Rodríguez-Beltrán J, Alonso N, Cantillon D, Costas C, et al. A non-canonical mismatch repair pathway in prokaryotes. Nat Commun 2017;8:14246.

[41] Makarov V, Manina G, Mikusova K, Möllmann U, Ryabova O, Saint-Joanis B, et al. Benzothiazinones kill Mycobacterium tuberculosis by blocking arabinan synthesis. Science 2009;324:801–4.
[42] Poce G, Bates RH, Alfonso S, Cocozza M, Porretta GC, Ballell L, et al. Improved BM212 MmpL3 inhibitor analogue shows efficacy in acute murine model of tuberculosis infection. PLoS One 2013;8:e56980.
[43] Mori G, Chiarelli LR, Esposito M, Makarov V, Bellinzoni M, Hartkoorn RC, et al. Thiophenecarboxamide derivatives activated by EthA kill Mycobacterium tuberculosis by inhibiting the CTP synthetase PyrG. Chem Biol 2015;22:917–27.
[44] Chiarelli LR, Mori G, Orena BS, Esposito M, Lane T, de Jesus Lopes, Ribeiro AL, et al. A multitarget approach to drug discovery inhibiting Mycobacterium tuberculosis PyrG and PanK. Sci Rep 2018;8:3187.
[45] Albesa-Jové D, Chiarelli LR, Makarov V, Pasca MR, Urresti S, Mori G, et al. Rv2466c mediates the activation of TP053 to kill replicating and non-replicating Mycobacterium tuberculosis. ACS Chem Biol 2014;9:1567–75.
[46] Mori G, Orena BS, Chiarelli LR, Degiacomi G, Riabova O, Sammartino JC, et al. Rv0579 is involved in the resistance to the TP053 antitubercular prodrug. Front Microbiol 2020;11:292.
[47] Neres J, Hartkoorn RC, Chiarelli LR, Gadupudi R, Pasca MR, Mori G, et al. 2-Carboxyquinoxalines kill Mycobacterium tuberculosis through noncovalent inhibition of DprE1. ACS Chem Biol 2015;10:705–14.
[48] Kapopoulou A, Lew JM, Cole ST. The MycoBrowser portal: a comprehensive and manually annotated resource for mycobacterial genomes. Tuberculosis 2011;91:8–13.
[49] Schildkraut JA, Coolen JPM, Burbaud S, Sangen JJN, Kwint MP, Floto RA, et al. RNA sequencing elucidates drug-specific mechanisms of antibiotic tolerance and resistance in Mycobacterium abscessus. Antimicrob Agents Chemother 2022;66:e0150921.
[50] Koul A, Vranckx L, Dhar N, Göhlmann HW, Özdemir E, Neefs JM, et al. Delayed bactericidal response of Mycobacterium tuberculosis to bedaquiline involves remodelling of bacterial metabolism. Nat Commun 2014;5:3369.
[51] McNeil MB, Ryburn HWK, Harold LK, Tirados JF, Cook GM. Transcriptional inhibition of the F1F0-type ATP synthase has bactericidal consequences on the viability of mycobacteria. Antimicrob Agents Chemother 2020;64 e00492-20.
[52] Klepp LI, Sabio y Garcia J, Bigi F. Mycobacterial MCE proteins as transporters that control lipid homeostasis of the cell wall. Tuberculosis 2022;132:102162.
[53] Santi I, Dhar N, Bousbaine D, Wakamoto Y, McKinney JD. Single-cell dynamics of the chromosome replication and cell division cycles in mycobacteria. Nat Commun 2013;4:2470.
[54] Dedrick RM, Smith BE, Cristinziano M, Freeman KG, Jacobs-Sera D, Belessis Y, et al. Phage therapy of mycobacterium infections: compassionate use of phages in 20 patients with drug-resistant mycobacterial disease. Clin Infect Dis 2023;76:103–12.
[55] Bhat ZS, Rather MA, Maqbool M, Lah HU, Yousuf SK, Ahmad Z. Cell wall: a versatile fountain of drug targets in Mycobacterium tuberculosis. Biomed Pharmacother 2017;95:1520–34.
[56] Machado D, Girardini M, Viveiros M, Pieroni M. Challenging the drug-likeness dogma for new drug discovery in tuberculosis. Front Microbiol 2018;9:383242.
[57] Dupont CL, Grass G, Rensing C. Copper toxicity and the origin of bacterial resistance – new insights and applications. Metallomics 2011;3:1109–18.
[58] Dalecki AG, Crawford CL, Wolschendorf F. Copper and antibiotics: discovery, modes of action, and opportunities for medicinal applications. Adv Microb Physiol 2017;70:193–260.
[59] Banaschewski B, Verma D, Pennings LJ, Zimmerman M, Ye Q, Gadawa J, et al. Clofazimine inhalation suspension for the aerosol treatment of pulmonary nontuberculous mycobacterial infections. J Cyst Fibros 2019;18:714–20.
[60] Pasca MR, Degiacomi G, Riabova O, Makarov V. Pyridine-2-thiol 1-oxide derivatives and their use for treatment of mammalian infections caused by mycobacterium or fungi. 2022 Italian patent application number P2245IT. PCT/EP2023/078712.
[61] Kwak N, Dalcolmo MP, Daley CL, Eather G, Gayoso R, Hasegawa N, et al. Mycobacterium abscessus pulmonary disease: individual patient data meta-analysis. Eur Respir J 2019;54:1801991.
[62] Wu ML, Aziz DB, Dartois V, Dick T. NTM drug discovery: status, gaps and the way forward. Drug Discov Today 2018;23:1502–19.
[63] Wu W, He S, Li A, Guo Q, Tan Z, Liu S, et al. A novel leucyl-tRNA synthetase inhibitor, MRX-6038, expresses anti-Mycobacterium abscessus activity in vitro and in vivo. Antimicrob Agents Chemother 2022;66:e0060122.
[64] Flores VD, Siqueira FD, Mizdal CR, Bonez PC, Agertt VA, Stefanello ST, et al. Antibiofilm effect of antimicrobials used in the therapy of mycobacteriosis. Microb Pathog 2016;99:229–35.
[65] Maggioncalda EC, Story-Roller E, Mylius J, Illei P, Basaraba RJ, Lamichhane G. A mouse model of pulmonary Mycobacteroides abscessus infection. Sci Rep 2020;10:3690.
[66] Silber N, Matos de Opitz CL, Mayer C, Sass P. Cell division protein FtsZ: from structure and mechanism to antibiotic target. Future Microbiol 2020;15:801–31.
[67] Andreu JM, Schaffner-Barbero C, Huecas S, Alonso D, Lopez-Rodriguez ML, Ruiz-Avila LB, et al. The antibacterial cell division inhibitor PC190723 is an FtsZ polymer-stabilizing agent that induces filament assembly and condensation. J Biol Chem 2010;285:14239–46.